ВЫСОКОКАЧЕСТВЕННАЯ ГЕНЕРАЦИЯ ПОЛОСОВЫХ ШАБЛОНОВ НА ОСНОВЕ ОПТИМИЗАЦИИ БИНАРНЫХ ПАТТЕРНОВ С ДЕФОКУСИРОВКОЙ

© 2017 г. X.-X. Li; Zh.-J. Zhang

Key Laboratory of Specialty Fiber Optics and Optical Access Networks, Shanghai University, Shanghai, China

Трехмерная реконструкция объектов в реальном времени находит все большее применение в различных областях. Это предъявляет повышенные требования к обычным методам, основанным на структурированном освещении, и в частности, к цифровой проекции полосовых шаблонов. Техника бинарной дефокусировки применительно к цифровой проекции полосовых шаблонов не только существенно повышает производительность системы при ее работе в реальном времени, но и существенно устраняет нелинейность проектора. Наилучшими среди прочих методов являются оптимизационные методы, основанные на размывании полос. Тем не менее, эти методы имеют два очевидных недостатка: целевая функция определяет сходство по общей интенсивности и игнорирует местные подобия, оптимизационная структура часто неэффективна или затратна по времени. В работе впервые предложена новая целевая функция, включающая член, отвечающий за общую интенсивность, и локальный структурный член, полностью оценивающий подобия. Далее, использована методология оптимизации, включающая гибридный оптимизационный алгоритм и подход полупериодной оптимизации. Преимущества предложенной целевой функции и оптимизационной методологии, а также улучшение качества и повышение скорости трехмерной реконструкции продемонстрированы как путем численного моделирования, так и экспериментально.

Ключевые слова: *трехмерная реконструкция, цифровая проекция полосовых шаблонов, техника бинарной дефокусировки, гибридный алгоритм "бинарный метод роя частиц – генетический алгоритм".*

HIGH-QUALITY FRINGE PATTERN GENERATION BASED ON BINARY PATTERN OPTIMIZATION WITH PROJECTOR DEFOCUSING

© 2017 X.-X. Li, Doctoral candidate of information science;
Z.-J. Zhang, Doctor of electronic science

Key Laboratory of Specialty Fiber Optics and Optical Access Networks, Shanghai University, Shanghai 200072, China

E-mail: megres.li@foxmail.com

The real-time three-dimensional reconstruction is increasingly important in many fields. However, it is a challenge for the conventional digital fringe projection technique. The binary defocusing technique applied to the digital fringe projection technique not only significantly improves the real-time performance but also fundamentally eliminates the nonlinearity of projector. In the existing techniques, the dithering techniques based on optimization are superior to the others. However, those optimization methods have two obvious drawbacks: the objective function just qualifies the global intensity similarity while ignores the local similarity, and the optimization framework is inefficient or time-consuming. This paper first presents a novel objective function consisting of a global intensity term and a local structure term to comprehensively evaluate similarity. Second, a model optimization framework, which includes a hybrid optimization algorithm and a half period optimization idea, is employed. Both simulations and experimental results show the advantages of the proposed objective function and the optimization framework, as well as the improvement of quality and speed of 3D reconstruction.

Keywords: *3D reconstruction, digital fringe projection, binary dithering technique, BPSO-GA hybrid algorithm.*

OCIS codes: 230.0230, 120.2830

Submitted 23.01.2016

1. Introduction

The development of the digital fringe projection (DFP) technique has been made in high-quality three-dimensional (3D) reconstruction thanks to the flexibility and simplicity of its system [1]. With the development of technical requirement of 3D reconstruction, the real-time performance is increasingly important [2]. To make sure of the real-time performance, we require a high measurement speed. However, it is a challenge for the conventional DFP technique. The main reason is that the maximum refresh rate of the typical projector is only 120 Hz when 8 bits gray sinusoidal pattern is projected [3]. In addition, the typical projector is usually a commercial device which is nonlinear for human vision. However, the nonlinearity can lead to the measurement error.

Several years ago, Texas Instruments developed an advanced technique which is able to reach a high speed when a binary pattern is projected. This breakthrough benefits from the digital mirror device (DMD) technique. For example, TI DLP Discovery D4100 projector can be set to 3.255×10^4 frame/s in binary mode with 1024×768 resolution [4]. Moreover, since the binary pattern only contains the white and black pixels, the nonlinear can be eliminated. Therefore, many researchers have utilized this performance to improve the DFP technique.

In 2009, S.Y. Lei and S. Zhang developed the technique in flexible 3D shape measurement using projector defocusing, which has successfully made rate breakthroughs [5]. However, the quality of its result is far worse than DFP technique due to the high-frequency harmonics influences. In 2010, some researchers introduced the pulse width modulate (PWM) techniques into binary defocusing technique [6, 7]. The high frequency harmonics can be easier to be eliminated, after defocusing. However, the technique also has the defects: (1) when the fringe stripes are wide, the improvements are limited [8], and (2) since the PWM technique is one-dimensional, it cannot be fully applied to the two-dimensional binary defocusing technique [9]. In 2012, W. Lohry and S. Zhang [10] proposed a technique to approximate the triangular waveform by modifying 2×2 pixels so that the result in patterns is better for the defocusing technique. However, if the fringe stripes are wide, it is difficult to achieve high-quality patterns.

Lately, some researchers developed the dithering techniques to generate the high-quality fringe pattern. Because the dithering techniques represent gray-scale images with binary images for printing and processing, it results in the higher quality of fringe pattern than other previous defocusing methods. The representative studies in this field include: Bayer method [11], error-diffusion method [12] and iteration method [13]. Generally speaking, the quality of pattern based on optimization is higher than that of other methods. For instance, the iteration method is an optimization method to minimize a norm function in the full-size pattern. However, the existing optimization methods have two main shortcomings: (1) the objective function of optimization just fits the global intensity similarity while ignores the influences of local structure similarity, and (2) the full-size optimization is time-consuming, and may be non-convergent or local convergent.

In this paper, we proposed a method to overcome the two shortcomings above. This method is a dithering method based on optimization, and it provides an approach to obtain the higher quality fringe pattern. This method includes two aspects. (1) A novel objective function containing a global similarity term and a local similarity term is proposed. The global similarity term is a full reference quality metric: normalized mean squared error (NMSE) and the local similarity term is a local structure quality metric: structural similarity index measure (SSIM).The novel objective function is minimized to make the defocused binary fringe pattern as close as possible to the ideal sinusoidal pattern. (2) A model optimization framework combining periodicity and symmetry of fringe pattern is employed. We use a hybrid algorithm including the binary particle swarm optimization (BPSO) and genetic algorithm (GA) to minimize the objective function. The hybrid algorithm can be called “BPSO-GA”. The algorithm can avoid the failure of the update rules in the standard algorithm (e.g. BPSO or GA). Considering the time-consuming, we only optimize the form of pixels in a half period using the periodicity and symmetry of sinusoidal fringe pattern, and adopt a parallel calculation method of BPSO-GA with GPU-accelerating. For verifying the effectiveness and accuracy of the proposed method, both simulations and experiments are made.

2. Principle

2.1. Three-step phase-shifting profilometry

The experimental setup is shown in Fig. 1, and we use the three-step phase-shifting algorithm to verify the performance of our proposed technique [14]. For this algorithm with a phase shift of $2\pi/3$, the fringe patterns can be described as

$$I_1(x,y) = a(x,y) + b(x,y)\cos[\varphi(x,y) - 2\pi/3], \quad (1)$$

$$I_2(x,y) = a(x,y) + b(x,y)\cos[\varphi(x,y)], \quad (2)$$

$$I_3(x,y) = a(x,y) + b(x,y)\cos[\varphi(x,y) + 2\pi/3], \quad (3)$$

where I is intensity, $a(x, y)$ is the average intensity, $b(x, y)$ is the intensity modulation, and $\varphi(x, y)$ is the phase which can be calculated with the following equation:

$$\varphi(x,y) = \tan^{-1}\frac{\sqrt{3}(I_1 - I_3)}{2I_2 - I_1 - I_3}. \quad (4)$$

Because of the characterization of $\tan^{-1}$, $\varphi(x, y)$ ranges from $-\pi$ to $+\pi$ and contains 2π discontinuity. That is to say, we need an unwrapping algorithm to remove the discontinuity. Actually, the purpose of the phase unwrapping is to obtain the true value of $n(x, y)$

$$\Phi(x,y) = \varphi(x,y) + 2\pi n(x,y), \quad (5)$$

where $\Phi(x, y)$ is the absolute unwrapped phase and the $n(x, y)$ is an integer which represents the order of the fringe at pixel (x, y). In our research, we use the exponential sequence temporal phase unwrapping algorithm, as introduced in paper [15].

The depth of the object $H(x, y)$ is deduced from the absolute unwrapped phase $\Phi(x, y)$.

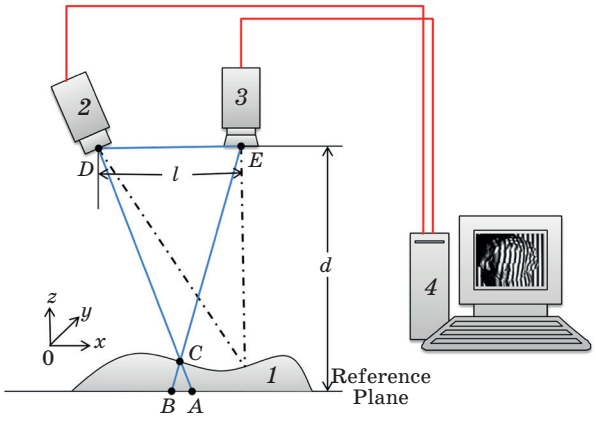

Fig. 1. The schematic experimental system for phase-shifting profilometry. *1* – object, *2* – DLP projector, *3* – CCD camera, *4* – computer.

In Fig. 1, because the points C on the object and A on the reference have the same phase value, we can get

$$\overline{AB} = \frac{\Phi_{CB}}{2\pi f} = \frac{\Phi_C - \Phi_B}{2\pi f}, \quad (6)$$

where the $\Phi_{CB} = \Phi_C - \Phi_B$ is the phase difference between points C and B, and f is the frequency of fringe. Moreover, due to the similarity of ΔABC and ΔCDE, $H(x, y)$ is described as follows:

$$H(x,y) = \frac{\overline{AB}(d/f)}{1 + \overline{AB}/l} = \frac{d\Phi_{CB}}{\Phi_{CB} + 2\pi lf}, \quad (7)$$

where d is the distance from the entrance pupil of camera to the reference plane and l is the distance between the exit pupil of the projector and the entrance pupil of camera.

2.2. Digital binary defocusing theory

Essentially, the defocusing effect can be viewed as convolution operation of binary pattern, and it can be written as

$$I(x,y) = G(x,y) \otimes I_d(x,y), \quad (8)$$

where $I(x, y)$ is the generated sinusoidal fringe pattern, $I_d(x, y)$ is the original binary pattern, $G(x, y)$ is the points spread function (PSF), and $\otimes$ represents convolution. The PSF is generally approximated by a circular Gaussian function [9]

$$G(x,y) = \frac{1}{2\pi\sigma^2}\exp\left(-\frac{x^2 + y^2}{2\sigma^2}\right), \quad (9)$$

where the standard deviation σ represents the defocusing level. In other words, the defocused optical system is a spatial two-dimensional (2D) low-pass filter. The smoothed binary pattern should be as close as possible to the continuous sinusoidal patterns. In general, the defocusing of binary pattern can be achieved by adjusting the focal distance of projector.

There are two obvious advantages using binary defocusing technique. (1) The projector's nonlinear gamma response can be removed. That is because the projector only generates the form of white and black rather than the form of gray. (2) A high measurement speed can be achieved. That is because the DMD component can generate a high refresh rate when the form of white and black (binary pattern) is projected.

3. Binary pattern construction framework

3.1. Objective function

The quality of sinusoidal fringe pattern plays a vital role in high-quality 3D reconstruction. In other words, the form of white and black pixels of binary pattern (before defocusing) directly influences the quality of sinusoidal fringe pattern (after defocusing). The purpose of optimization should be as close as possible to the ideal sinusoidal pattern through altering the form of white or black pixels. The existing utilized objective function is often described as a norm function, such as the frobenius norm function [16]

$$\min_{B,G}\left\|I(x,y)-G(x,y)\otimes I_d(x,y)\right\|_F, \qquad (10)$$

where $\|\cdot\|_F$ is the frobenius norm, $I(x, y)$ is an ideal sinusoidal pattern, $G(x, y)$ represents a 2D Gaussian kernel, $I_d(x, y)$ is a binary pattern, and $\otimes$ represents convolution. Obviously, this function has clear physical meanings and is mathematically easy in the optimization. But it only relates to the similarity of global intensity between the ideal sinusoidal fringe pattern and its corresponding binary pattern. That is to say, the similarity of local structure is ignored while it is also very important.

Considering the shortcoming above, we construct a novel objective function, which consists of two terms: a global intensity term and a local structure term. The objective function can be described as

$$\begin{aligned} Obj(I,I_d) = w_n Global(I,I_d) + \\ + (1-w_n)[1-Local(I,I_d)]. \end{aligned} \qquad (11)$$

In Eq. (11) the corresponding dithered pattern I_d, which is given by an ideal sinusoidal fringe pattern I, is obtained by minimizing the equation. $Global(I, I_d)$ and $Local(I, I_d)$ measure the global similarity and the local similarity, respectively. The w_n is the weighting factor limited in [0, 1] and we set $w_n = 0.7$.

a. Global intensity similarity

In Eq. (11) the essence of $Global(I, I_d)$ is a full reference quality metric: normalized mean squared error (NMSE). It has a range in [0, 1] and can be described as

$$Global(I,I_d) = \frac{\sum_H \sum_W [I-G(I_d)]^2}{\sum_H \sum_W (I)^2}, \qquad (12)$$

where H and W respectively represent two directions of the image coordinate. I represents the ideal sinusoidal fringe pattern and $G(I_d)$ represents a Gaussian filtered binary dithered pattern.

b. Local structure similarity

To evaluate the local structure similarity, we employ $Local(I, I_d)$ in Eq. (11). The essence of this term is the structural similarity index measure (SSIM) [17]. In SSIM system, since the structure information is independent of the average luminance and contrast information, the influence of the illumination in an image needs to be separated. The system diagram of the SSIM is shown in Fig. 2.

According to the image signal theory, the two image signals I and I_d are input into the SSIM system through two signal channels. The signal I is the ideal sinusoidal fringe pattern, which can serve as quantitative measurement of the quality of the other signal. Meanwhile, the signal I_d is the corresponding binary dithered pattern. For measurement and comparison, the signal I_d should be Gaussian filtered. The smoothed pattern can be described as $II = G(I_d)$.

The SSIM measures the local structure similarity in a local neighborhood. And then, the SSIM system separates similarity measurement into three comparisons: luminance, contrast and

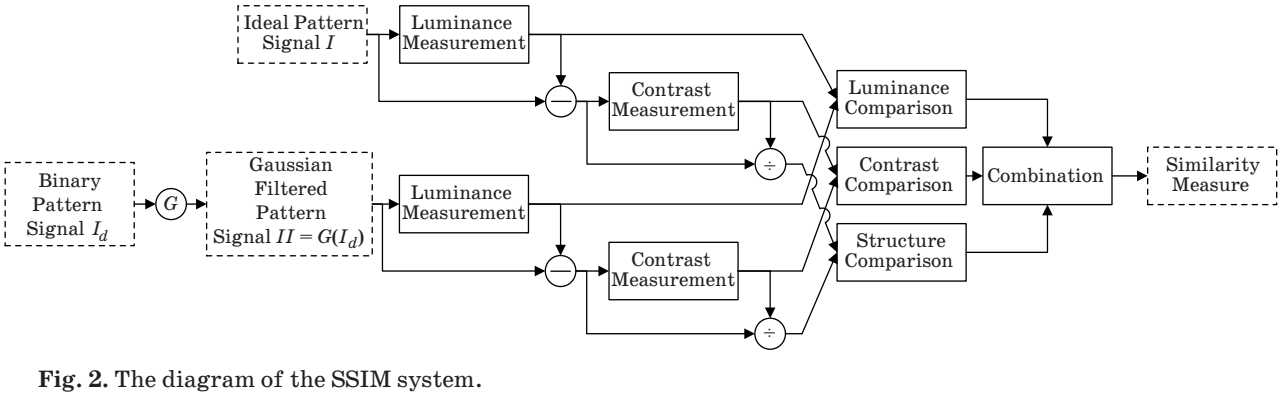

Fig. 2. The diagram of the SSIM system.

structure. We assume that the I and II all have N elements. It is noted that the x in the following equations represents the signal I or II for simplified representation.

First, the luminance of each signal is compared. The luminance is estimated as the mean intensity

$$\mu_x = \frac{1}{N}\sum_{i=1}^{N} x_i, \quad x = I \text{ or } II. \tag{13}$$

Therefore, the luminance comparison function $l(I, II)$ can be defined as a function of μ_I and μ_{II}, and is shown in Eq. (14)

$$l(I, II) = \frac{2\mu_I\mu_{II} + c_1}{\mu_I^2 + \mu_{II}^2 + c_1}, \tag{14}$$

where the c_1 is a small constant to avoid singularity (specially, we set $c_1 = 1$).

Second, the mean intensity μ_x should be removed from the signal. The resulting signal is $x - \mu_x$, $x = I$ or II. Thus, the signal contrast is estimated as the standard deviation. The function is defined by

$$\sigma_x = \sqrt{\frac{1}{N-1}\sum_{i=1}^{N}(x_i - \mu_x)^2}, \quad x = I \text{ or } II. \tag{15}$$

The contrast comparison function $c(I, II)$, which has the similar form with $l(I, II)$, is a function of σ_I and σ_{II}, as shown in Eq. (16)

$$c(I, II) = \frac{2\sigma_I\sigma_{II} + c_2}{\sigma_I^2 + \sigma_{II}^2 + c_2}, \tag{16}$$

where the c_2 is a small constant to avoid singularity (specially, we set $c_2 = 1$).

Third, the signal is normalized by its own standard deviation, and the correlation of the normalized signal $(x - \mu_x)/\sigma_x$, $x = I$ or II is equivalent to the correlation coefficient between the signal I and II. In other words, the correlation between the images is used as a simple and effective measure to quantify the structural similarity. Thus, the structure comparison function $s(I, II)$ is a function of σ_I, σ_{II} and $\sigma_{I,II}$. The function is shown in Eq. (17)

$$s(I, II) = \frac{\sigma_{I,II} + c_3}{\sigma_I + \sigma_{II} + c_3}. \tag{17}$$

Similarly, we also set a small constant c_3 to avoid singularity (specially, we set $c_3 = 1$). The standard deviation $\sigma_{I,II}$ is solved for

$$\sigma_{I,II} = \frac{1}{N-1}\sum_{i=1}^{N}(I_i - \mu_I)(II_i - \mu_{II}). \tag{18}$$

Finally, the Eqs. 14, 16 and 17 are combined by weighting multiplication to generate an overall similarity measurement, as shown in Eq. 19

$$Local(I, I_d) = l\left[I, G(I_d)\right]^{\alpha} c\left[I, G(I_d)\right]^{\beta} s\left[I, G(I_d)\right]^{\gamma}, \tag{19}$$

where α, β and γ are used to adjust the weightiness of the three components. Specially, α, β and γ are all set to 1.

3.2. Optimization framework

As the existing objective function, the form of white and black pixels in the full-sized binary pattern is optimized. The purpose of the optimization is to generate a "good" binary dithered pattern, which after defocusing (e.g. applying a Gaussian filter) approximates to the ideal sinusoidal fringe pattern. In the employed framework, because of the periodicity and symmetry of fringe pattern, we just optimize in a half period, and then tile the "best" half period to generate a full-size pattern. For faster convergence, the initial pattern is a half period of square wave pattern. The periodicity and phase of the square wave pattern are the same as the sinusoidal pattern.

We minimize the objective function using a model optimization algorithm BPSO-GA, which combines the features of BPSO and GA. The BPSO-GA can avoid that the updating rules do not work well in the standard algorithm

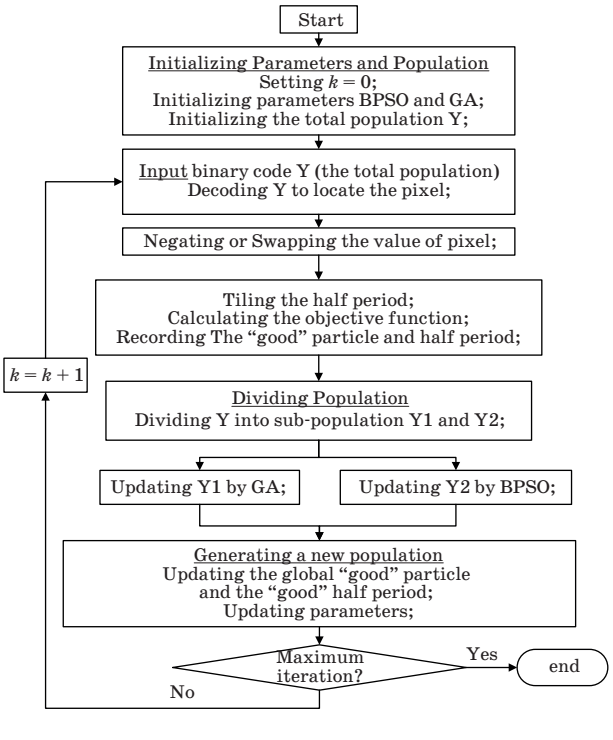

Fig. 3. Optimization flowchart.

(e.g. BPSO or GA) [18]. In consideration of time-consuming, a parallel calculation method with GPU-accelerating is adopted [19].

In the employed BPSO-GA algorithm, the particle is a binary code, which represents the coordinate of the current pixel. The pixel is altered in its 3×3 neighborhood window. There are two altering rules: (1) the pixel is mutated to its opposite status, and (2) the pixel swaps with its 4 or 8 neighbor pixels. We divide the total population Y into two sub-populations: Y1 and Y2. The sub-population Y1 is updated by selection, crossover and mutation probability in GA algorithm. Meanwhile, the sub-population Y2 is updated by position and velocity equation in BPSO algorithm. The flowchart of the model algorithm is shown in Fig. 3.

4. Simulations

In this section, we verify the effectiveness and accuracy of the proposed method through the following four simulation cases.

Case 1 proves our proposed objective function, compared with the norm function. These two objective functions are optimized with the same optimization method and conditions. Moreover, the Gaussian filter (5×5 pixels with a standard deviation of 5/3 pixels) is used for smoothing. The size of the figure is 400×400 pixels and the fringe period is 20 pixels. We chose the cross sections with the same row as the object of study. The intensity difference and the phase difference of cross sections are compared respectively. For the intensity difference, the mean value and the standard deviation value of our proposed objective function (mean = 0.0669 and standard deviation = 3.3707) are both less than the results of the norm function (mean = 1.2054 and standard deviation = 5.3907). For the phase difference, Similarly, our proposed function has the smaller phase RMS error (proposed function: 0.0051 rad, and norm function: 0.0065 rad). By statistical analysis above, it is clear that our proposed objective function is more effective than the norm function.

Case 2 verifies that our proposed method to generate high-quality fringe pattern is more effective than the existing methods. The existing methods include: Bayer method [11], error-diffusion method [12] and iteration method [13]. In this case, the existing methods and our proposed method generate the binary dithered patterns, and then these patterns are blurred by the same Gaussian filter (5×5 pixels with a standard deviation of 5/3 pixels). The size of each pattern is 100×100 pixels, and the fringe period is 64 pixels. We analyzed the intensity difference of the cross sections, and table shows the mathematical statistics. We find the mean value and the standard deviation value of our proposed method are both less than the results of other methods. It means that our proposed method is closer to the ideal pattern than other methods.

The statistics of the intensity difference of the cross sections

Method	Mean	Standard Deviation
Bayer	3.1386	8.4036
Error Diff.	1.3960	3.7419
Iteration	0.1386	3.0953
Proposed	0.1188	2.8576

Case 3 contains two tasks. The first task is that we used the various methods to generate fringe patterns with a wide range of fringe stripe breadths (32, 64, 96, 128, 160, 192, 224 and 256 pixels). Furthermore, the smoothed patterns are generated by a Gaussian filter (5×5 pixels with a standard deviation of 5/3 pixels). The second task is that we used the various methods to generate fringe patterns with a wide range of Gaussian filter sizes (5, 7, 9, 11 and 13 pixels, for level 1 through 5). The values of standard deviation are all 5/3 pixels. This task is accomplished when the fringe period is 32 (T = 32) pixels and 96 (T = 96) pixels. The size of each pattern is 256×256 pixels in two tasks.

Since our proposed $Obj(I, I_d)$ function contains the global term and local term, as well as case 1 has verified its improvement, we utilize $Obj(I, I_d)$ as a quality evaluation index. Figure 4 shows the results of the first task. Specifically, Fig. 4 shows that (*1*) the $Obj(I, I_d)$ value of each method has a growth trend except Bayer method, (*2*) this clearly shows that our proposed method works the best when iteration method works better than error-diffusion method, and (3) it is noticed that the trend of Bayer method is unstable when the fringe stripe grows. Figure 5 shows the results of the second task. Figure 5a represents T = 32 pixels and Fig. 5b represents T = 96 pixels. Specifically, Fig. 5 shows that (*1*) the $Obj(I, I_d)$ value of each method reduces when increasing the amount of defocusing for T = 32 and 96 pixels, (*2*) it is clear that our proposed method works the best

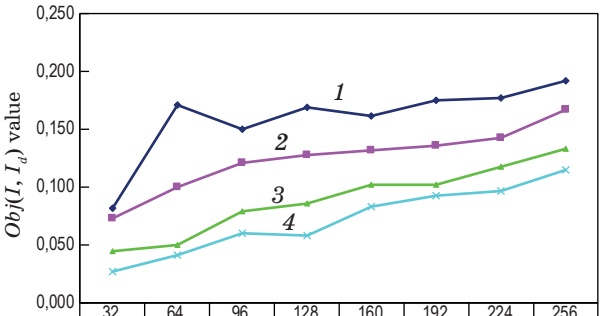

	32	64	96	128	160	192	224	256
1	0,082	0,171	0,150	0,169	0,162	0,175	0,177	0,192
2	0,073	0,100	0,121	0,128	0,132	0,136	0,143	0,167
3	0,045	0,050	0,079	0,086	0,102	0,102	0,118	0,133
4	0,027	0,041	0,060	0,058	0,083	0,093	0,097	0,115

Fringe pitch, pixels

Fig. 4. Comparison of the different dithering method with a range of fringe stripe breaths. *1* – Bayer, *2* – error diff., *3* – iteration, *4* – proposed.

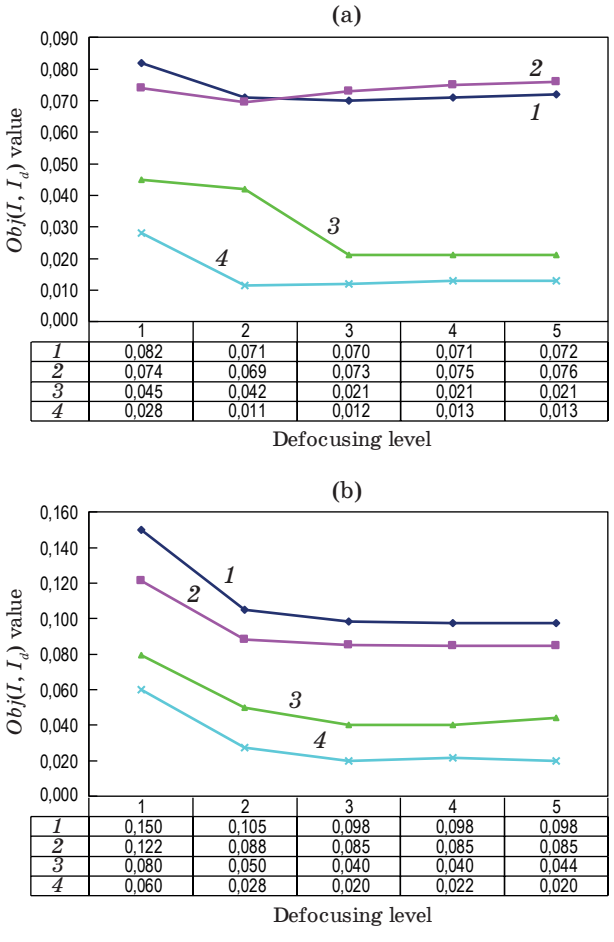

	1	2	3	4	5
1	0,082	0,071	0,070	0,071	0,072
2	0,074	0,069	0,073	0,075	0,076
3	0,045	0,042	0,021	0,021	0,021
4	0,028	0,011	0,012	0,013	0,013

Defocusing level

	1	2	3	4	5
1	0,150	0,105	0,098	0,098	0,098
2	0,122	0,088	0,085	0,085	0,085
3	0,080	0,050	0,040	0,040	0,044
4	0,060	0,028	0,020	0,022	0,020

Defocusing level

Fig. 5. The $Obj(I, I_d)$ value with varying amount of defocusing by simulations. (a) Fringe patterns ($T = 32$). (b) Fringe patterns ($T = 96$). *1* – Bayer, *2* – error diff., *3* – iteration, *4* – proposed.

when increasing the amount of defocusing for $T = 32$ and 96 pixels, and (*3*) when the defocusing level exceeds *3*, the $Obj(I, I_d)$ value is prone to stability. In a word, our proposed method works better than other previously proposed methods when the fringe stripe breadth or defocusing level is changed.

In case *4*, we simulated a 3D shape, as shown in Fig. 6a. Since Eq. (7) can be approximated as a linear relation, we set $\varphi = 0.2h$ (h represents the depth of the 3D shape and φ represents the phase of the phase-shifted fringe pattern). Therefore, the depth map of the 3D shape can be encoded by the blurred binary patterns generated by various methods. The kernel of Gaussian filter is 5×5 and its standard deviation is 5/3 pixels. An example of Bayer method is shown in Fig. 6b. Furthermore, we recovered the depth profile, and the recovered example of Bayer method is shown in Fig. 6c. Through statistical analysis, the standard deviation of depth error with Bayer method, error-diffusion method, iteration method, and our proposed method respectively are 0.0481, 0.0267, 0.0209, and 0.0128 mm. The improvement is substantial: the depth error with our proposed method is reduced to 0.0128 mm. Seen from the reconstruction results and the statistical analysis of the depth error, once again, our proposed method can produce the better result.

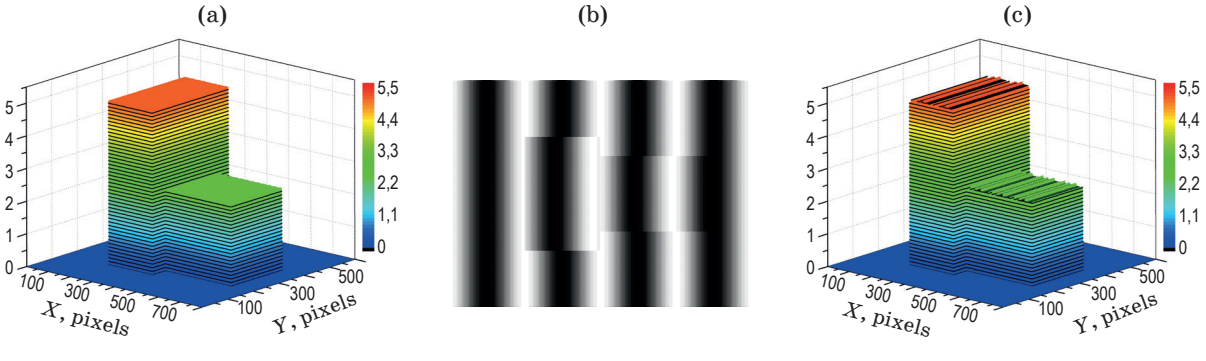

Fig. 6. The simulation of a 3D shape. (a) The 3D profile. (b) One of the blurred binary patterns with Bayer method. (c) The 3D reconstructed result with Bayer method.

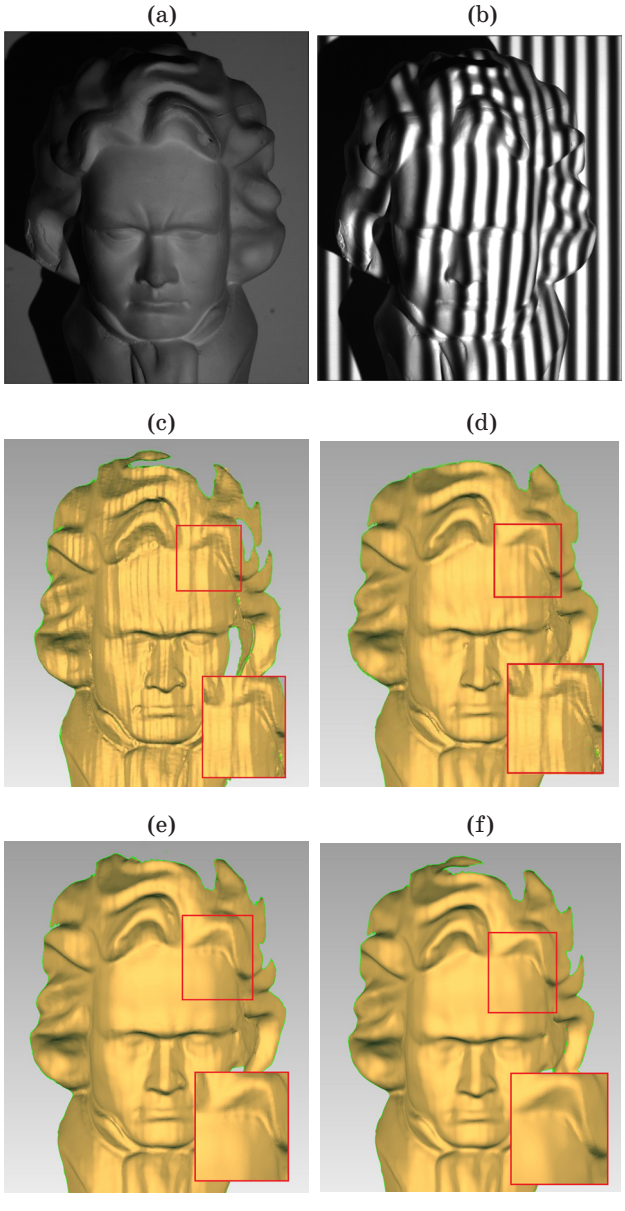

Fig. 7. The reconstructions of the Beethoven head. (a) Photo of the Beethoven head. (b) One of the binary patterns. (c–f) The 3D result with Bayer method, error diffusion method, iteration method and our proposed method.

5. Experiments

We built a 3D shape reconstruction system to verify the performance of our proposed method. The system includes a DLP projector (model: Vivitek D555WH) and a charge-coupled-device (CCD) camera (model: DALSA DS-24-02M30). We chose the camera resolution of 800×600 for all the tests. The DLP projector has 1024×768 native resolution with 1.0 m projection distance. The model of camera lens is Kowa LM25HC, which has a 25 mm focal length. The level of defocusing was realized by manually adjusting the focal distance of the projector. It is necessary to note that the 3D data need to be smoothed by Gaussian filter to reduce the random noise.

Firstly, a white flat board was measured. The unwrapped phases are obtained by various methods. Meanwhile, the phase error of each method is obtained. The standard deviation value of the phase error by Bayer method, error-diffusion method, iteration method, and our proposed method respectively are 0.0630, 0.0445, 0.0408 and 0.0332 rad. Seen from the statistical result, our proposed method generated the best result when the Bayer method performed worst.

Secondly, we measured a more complex 3D shape, Beethoven Head, shown in Fig. 7a. The captured binary pattern which is distorted by the profile of the statue, shown in Fig. 7b, clearly shows that the projector was nearly focused. Figure 7c–f respectively shows the reconstruction results with Bayer method, error-diffusion method, iteration method, and our proposed method. Seen from the figures of partial enlargement, it clearly shows the improvement of our proposed method over other methods.

6. Conclusion

This paper has presented a novel 3D shape reconstruction technique using the binary dithered patterns based on optimization and the phase-shifting profilometry. This method improves two shortcomings of the existing dithering technique based on optimization: (1) the objective function ignores the evaluation of local similarity, and (2) the optimization framework is inefficient or time-consuming. Both simulation and experimental results have demonstrated the success of our proposed method.

* * * * *

REFERENCES

1. *Geng J.* Structured-light 3D surface imaging: a tutorial // Adv. Opt. Photonics. 2011. V. 3. № 2. P. 128–160.
2. *Karpinsky N., Zhang S.* High-resolution, real-time 3D imaging with fringe analysis // J. Real-Time Image Pr. 2012. V. 7. № 1. P. 55–66.
3. *Zhang S.* Recent progresses on real-time 3-D shape measurement using digital fringe projection techniques // Opt. Laser Eng. 2010. V. 48. № 2. P. 149–158.
4. *Zhang Z.H.* Review of single-shot 3D shape measurement by phase calculation-based fringe projection techniques // Opt. Laser Eng. 2012. V. 50. P. 1097–1106.
5. *Lei S.Y., Zhang S.* Flexible 3-D shape measurement using projector defocusing // Opt. Lett. 2009. V. 34. № 20. P. 3080–3082.
6. *Ayubi G.A., Ayubi J.A., Martino Di J.M., Ferrari J.A.* Pulse-width modulation in defocused three-dimensional fringe projection // Opt. Lett. 2010. V. 35. № 21. P. 3682–3684.
7. *Wang Y., Zhang S.* Optimal pulse width modulation for sinusoidal fringe generation with projector defocusing // Opt. Lett. 2010. V. 35. № 24. P. 4121–4123.
8. *Wang Y., Zhang S.* Comparison of the squared binary, sinusoidal pulse width modulation, and optimal pulse width modulation methods for three-dimensional shape measurement with projector defocusing // Appl. Opt. 2012. V. 51. № 7. P. 861–872.
9. *Zuo C., Chen Q., Feng S., Feng F., Gu G., Sui X.* Optimized pulse width modulation pattern strategy for three-dimensional profilometry with projector defocusing // Appl. Opt. 2012. V. 51. № 19. P. 4477–4490.
10. *Lohry W., Zhang S.* 3D shape measurement with 2D area modulated binary patterns // Opt. Laser Eng. 2012. V. 50. № 7. P. 917–921.
11. *Wang Y.J., Zhang S.* Three-dimensional shape measurement with binary dithered patterns // Appl. Opt. 2012. V. 51. № 27. P. 6631–6636.
12. *Li B.W., Wang Y.J., Dai J.F., Lohry W., Zhang S.* Some recent advances on superfast 3D shape measurement with digital binary defocusing techniques // Opt. Laser Eng. 2014. V. 54. P. 236–246.
13. *Dai J.F., Zhang S.* Phase-optimized dithering technique for high-quality 3D shape measurement // Opt. Laser Eng. 2013. V. 51. № 6. P. 790–795.
14. *Huang P.S., Zhang S.* Fast three-step phase-shifting algorithm // Appl. Opt. 2006. V. 45. № 21. P. 5086–5091.
15. *Huntley J.M., Saldner H.O.* Shape measurement by temporal phase unwrapping: Comparison of unwrapping algorithms // Meas. Sci. Technol. 1997. V. 8. № 9. P. 986–992.
16. *Dai J.F., Li B.W., Zhang S.* High-quality fringe pattern generation using binary pattern optimization through symmetry and periodicity // Opt. Laser Eng. 2014. V. 52. P. 195–200.
17. *Wang Z., Bovik A.C., Sheikh H.R., Simoncelli E.P.* Image quality assessment: From error visibility to structural similarity // IEEE T. Image Process. 2004. V. 13. № 4. P. 600–612.
18. *Chen X.X., Qiu J., Liu G.J.* Optimal test selection based on hybrid BPSO and GA // Chinese J. Sci. Instrum. 2009. V. 30. № 8. P. 1674–1680.
19. *Roberge V., Tarbouchi M., Okou F.* Collaborative parallel hybrid metaheuristics on graphics processing unit // Int. J. Comp. Intel. & Appl. 2015. V. 14. № 1. P. 1–16.